Higher perfusion of rectum carcinoma relative to tumor-free rectal wall: quantification by a new imaging biomarker diffusion-derived vessel density (DDVD)

Bao-Lan Lu[1#], Dian-Qi Yao[2#], Yì Xiáng J. Wáng[2], Zhi-Wen Zhang[1], Zi-Qiang Wen[1], Ben-Heng Xiao[2], Shen-Ping Yu[1]

[1]Department of Radiology, The First Affiliated Hospital, Sun Yat-Sen University, Guangzhou, China; [2]Department of Imaging and Interventional Radiology, Faculty of Medicine, The Chinese University of Hong Kong, Shatin, New Territories, Hong Kong SAR, China

Contributions: (I) Conception and design: BL Lu, DQ Yao, YXJ Wáng, SP Yu; (II) Administrative support: BL Lu, SP Yu; (III) Provision of study materials or patients: BL Lu, BH Xiao, SP Yu; (IV) Collection and assembly of data: BL Lu, ZW Zhang, ZQ Wen, SP Yu; (V) Data analysis and interpretation: BL Lu, DQ Yao, YXJ Wáng; (VI) Manuscript writing: All authors; (VII) Final approval of manuscript: All authors.

#These authors contributed equally to this work.

Correspondence to: Shen-Ping Yu, MD. Department of Radiology, The First Affiliated Hospital, Sun Yat-Sen University, No. 135, Xingang Xi Road, Guangzhou, China. Email: yushp@mail.sysu.edu.cn; Yì Xiáng J. Wáng, MD. Department of Imaging and Interventional Radiology, Faculty of Medicine, The Chinese University of Hong Kong, Shatin, 30-32 Ngan Shing Street, Shatin, New Territories, Hong Kong SAR, China. Email: yixiang_wang@cuhk.edu.hk.

Background: Diffusion-derived vessel density (DDVD) is a physiological surrogate of the area of micro-vessels per unit tissue area. DDVD is calculated according to: $DDVD(b0b5) = Sb0/ROIarea0 - Sb5/ROIarea5$, where $Sb0$ and $Sb5$ refer to the tissue signal when b is 0 or 5 s/mm^2. This study applied DDVD to assess the perfusion of rectal carcinoma (RC).

Methods: MRI was performed with a 3.0-T magnet. Diffusion weighted image with b-values of 0, 5 s/mm^2 were acquired in 113 patients with non-mucinous RC and 15 patients with mucinous RC. Diffusion-derived vessel density ratio [DDVDr(b0b5)] was DDVD(b0b5) of RC divided by DDVD(b0b5) of tumor-free rectal wall.

Results: The median value of the DDVDr(b0b5) for non-mucinous RCs was 1.430, with the majority of RCs showing a higher DDVD than the adjacent tumor-free wall [i.e., with DDVDr(b0b5) >1]. 90.3% (102/113) of non-mucinous RCs were hypervascular, 1.77% (2/113) were iso-vascular, and 7.96% (9/113) were hypovascular. The median value of the DDVDr(b0b5) for mucinous RCs was 1.660. 73.3% (11/15) of mucinous RCs were hypervascular, and 26.7% (4/15) were hypovascular. A trend (P=0.09) was noted that earlier clinical grades non-mucinous RCs had a higher DDVDr(b0b5) than those of the advanced clinical grades (2.245 for grade 0&I, 1.460 for grade II, 1.430 for grade III, 1.130 for grade IV). A non-significant trend was noted with well and moderately differentiated non-mucinous RCs had a higher DDVDr(b0b5) than that of poorly differentiated non-mucinous RCs (median: 1.460 *vs.* 1.320). A non-significant trend was noted with MRI-detected extramural vascular invasion (mrEMVI) positive non-mucinous RCs had a higher DDVDr(b0b5) than that of mrEMVI negative non-mucinous RCs (1.630 *vs.* 1.370).

Conclusions: DDVD results in this study approximately agree with contrast agent dynamically enhanced CT literature data.

Keywords: Rectal carcinomas (RCs); perfusion; diffusion-weighted imaging (DWI)

Introduction

Rectal carcinoma (RC) is one of the most common malignant tumors in the world. Despite the progress in RC screening programs and treatment, the 5-year overall survival remains low. The prognosis of primary RC is associated with clinical staging and the differentiation degree. Imaging is vital in diagnostic workup, therapeutic planning, and monitoring. Angiogenesis plays an important role in the process of growth and metastasis of solid tumors and is a useful prognostic marker in almost all carcinomas, including colorectal cancer (1-3). An *in vivo* marker of RC angiogenesis is valuable for diagnosis, risk stratification, and monitoring of therapeutic success in RC patients. Numerous imaging studies have been conducted to study the perfusion status of RC, with the common modalities including dynamic contrast enhanced (DCE) CT (4-6), DCE MRI (7,8), intravoxel incoherent motion (IVIM) MRI (9,10). RCs mostly show higher perfusion values compared with the adjacent normal rectal wall. Studies have also investigated the potential correlation of quantitative parameters derived from imaging with angiogenesis and biological aggressiveness of RC.

On diffusion-weighted imaging (DWI), blood vessels (including micro-vessels) show high signal when there is no motion probing gradient (MPG, b=0 s/mm^2), while they show low signal even when very low b-values (such as b=1 or 2 s/mm^2) are applied. Thus, the signal difference between images when the motion probing gradient is off and images when the motion probing gradient is on reflects the extent of tissue vessel density. Recently, Wáng proposed that liver tissue micro-perfusion can be measured by a DWI-derived surrogate biomarker (DDVD: diffusion-derived vessel density) (11):

$$DDVD(b0b2) = Sb0/ROIarea0 - Sb2/ROIarea2$$
$$\left[\text{unit: arbitrary unit (au)/pixel} \right] \quad [1]$$

where ROIarea0 and ROIarea2 refer to the number of pixel in the selected region-of-interest (ROI) on b=0 s/mm^2 and b=2 s/mm^2 images, respectively. Sb0 refers to the measured total liver signal intensity within the ROI when b=0 s/mm^2, and Sb2 refers to the measured total liver signal intensity within the ROI when b=2 s/mm^2, thus Sb/ROIarea equates to the mean signal intensity within the ROI. Sb2 and ROIarea2 can also be approximated by other low b-value diffusion image data.

DDVD can be interpreted as a physiological surrogate of the area of micro-vessels per unit tissue area, which can be conceptually converted to a surrogate of the volume of micro-vessels per tissue unit volume if multiple slices are integrated. The clinical usefulness of DDVD as a straightforward diffusion imaging biomarker has been recently demonstrated (11-18). DDVD is a useful parameter for the distinguishing of livers with and without fibrosis, and livers with severer fibrosis tend to have even lower DDVD measurements than those with milder liver fibrosis (11-13). Zheng *et al.* (14) described spleen DDVD is decreased in viral hepatitis-b liver fibrosis patients. Huang *et al.* (15) showed that DDVD analysis demonstrates liver parenchyma has an age-dependent decrease of micro-perfusion. This agrees with the known physiological age-dependent reduction in liver blood flow which has been well documented using a variety of technical methods including histology, dye dilution, and indicator clearance. Pathohistological studies and contrast-enhanced CT/MRI data showed higher blood volume in HCC relative to native liver tissue. Li *et al.* (16) applied DDVD to assess the perfusion of hepatocellular carcinoma (HCC). DDVD results (ratio of HCC DDVD to background liver DDVD equals around 3.0) approximately agreed with contrast agent dynamically enhanced CT/MRI literature data (19,20), whereas DDVD results differ from earlier IVIM study results where HCC perfusion fraction (PF) was paradoxically lower relative to native liver tissue (16). Li *et al.* also demonstrated a slightly higher DDVD value for microvascular invasion positive HCCs than for microvascular invasion negative HCCs, and a slightly higher DDVD value for more malignment HCCs than for better differentiated HCCs. On the other hand, earlier IVIM studies demonstrated slightly lower perfusion measures for MVI(+) HCCs or more malignment HCCs. He *et al.* (17) reported that DDVD analysis of the placenta allowed excellent separation of normal and early preeclampsia pregnancies. More recently, Lu *et al.* (18) reported that DDVD was significantly higher in pregnant women with placenta accreta spectrum disorders than women with normal placenta, and especially higher in patients with placenta increta and percreta.

The analysis of DDVD requires only two b-values (with one being b=0 s/mm^2), allowing a significantly shorter scanning time than DCE CT/MRI or IVIM imaging. Such a protocol can be completed within a signal breath-hold duration, which renders it useful when the target organ is subject to respiratory motion. Compared with contrast agent DCE imaging, DDVD protocol does not involve contrast injection, data acquisition is much faster, and data post-processing is also relatively straightforward. This study
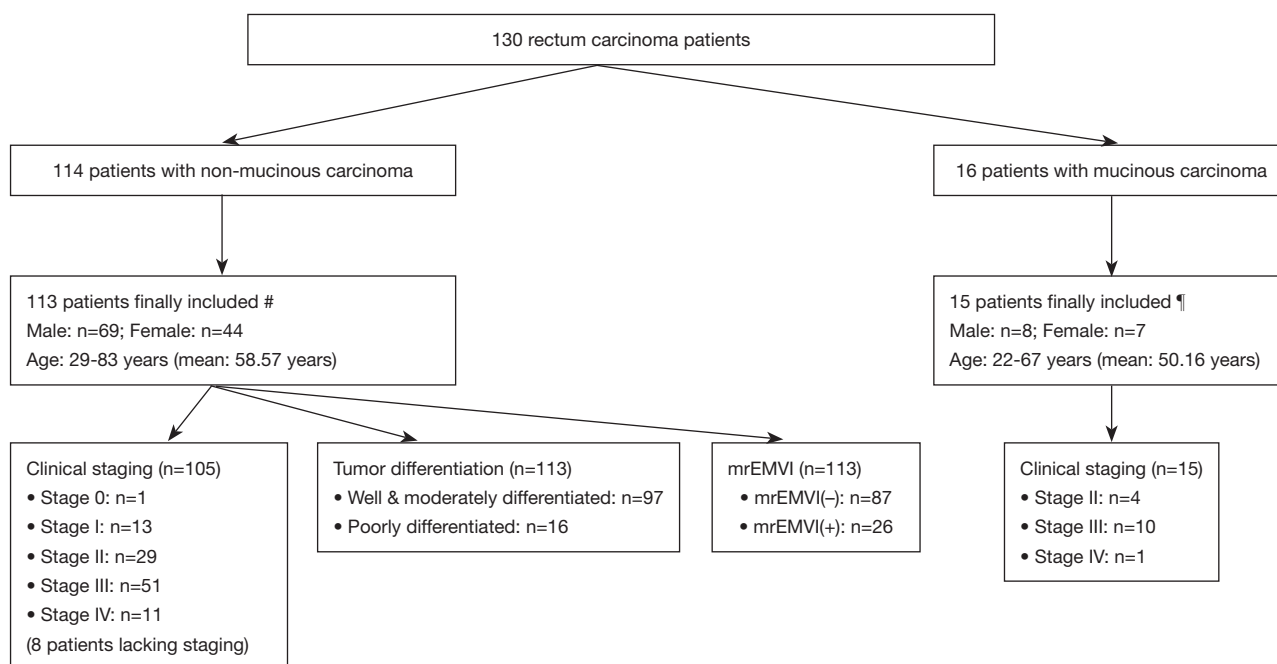
Figure 1 Flow diagram of patient inclusion. #, in one patient, tumor-free rectal signals at b=5/10 images were higher than tumor-free rectal wall at b=0 images. MRI signal is not always stable and can be affected by many factors including motion artifacts and scaling factor. Data of this patient was excluded from analysis; ¶, one patient did not have tumor-free rectal wall, and this patient was excluded from analysis. In mucinous carcinoma group, three cases were MRI-detected extramural vascular invasion positive. mrEMVI, MRI-detected extramural vascular invasion; MRI, magnetic resonance imaging.

evaluates the potential applications of DDVD to assess the perfusion of RC.

Methods

The study was conducted in accordance with the Declaration of Helsinki (as revised in 2013). The conduct of the study was approved by the local institutional ethical committee, and informed consent was obtained for all study subjects. All patients had primary RC with surgical pathology or biology confirmation. We excluded: (I) recurrent carcinoma; (II) neoadjuvant therapy was administered before MR examination; (III) the tumor did not have a sufficiently large parenchyma area for selecting ROIs (for all included tumors, longitudinal length was >13 mm and axial area was >230 mm^2 in the largest plane). We enrolled 130 patients (with two patients later excluded for analysis), their clinical staging (21), histological grading (22), MRI-detected extramural vascular invasion (mrEMVI, Figures S1,S2) (23,24), are shown in *Figure 1*. Non-mucinous carcinoma and mucinous carcinoma were separately grouped due to the different biological behaviours of these two groups of

tumors. Mucinous carcinoma is characterized by abundant extracellular mucin that constitutes more than 50% of the tumor volume. Mucinous RC is related to a lower response rate to chemoradiotherapy, and poorer prognosis compared to non-mucinous RC, even when corrected for clinical stage (25).

The rectal MR examination was performed using a 3.0T MRI scanner (Magnetom Verio; Siemens Healthcare, Erlangen, Germany) equipped with an 8-channel body-matrix coil. All patients were routinely intramuscularly injected with 20 mg of Anisodamine to minimize intestinal peristaltic movement. Prior to the initial MRI scan, 30–120 mL of ultrasound gel was injected into the rectum to make the boundary of tumor displayed more clearly. In addition to standard rectal MRI (10), a single-shot spin-echo echo-planar-imaging sequence IVIM-DWI sequence was sampled prior to any gadolinium injection. Scan parameters included: TR/TE, 3,800/74.7 ms; FOV 300×245 mm; 6 mm slice thickness; inter-slice gap: 0.6 mm; voxel size 2.7×2.7×6.0 mm; signal averaging =2. A total of 16 b-values (0, 5, 10, 20, 30, 40, 60, 80, 100, 150, 200, 400, 600, 1,000, 1,500, 2,000 s/mm^2) were applied. Standardly 21 slices were
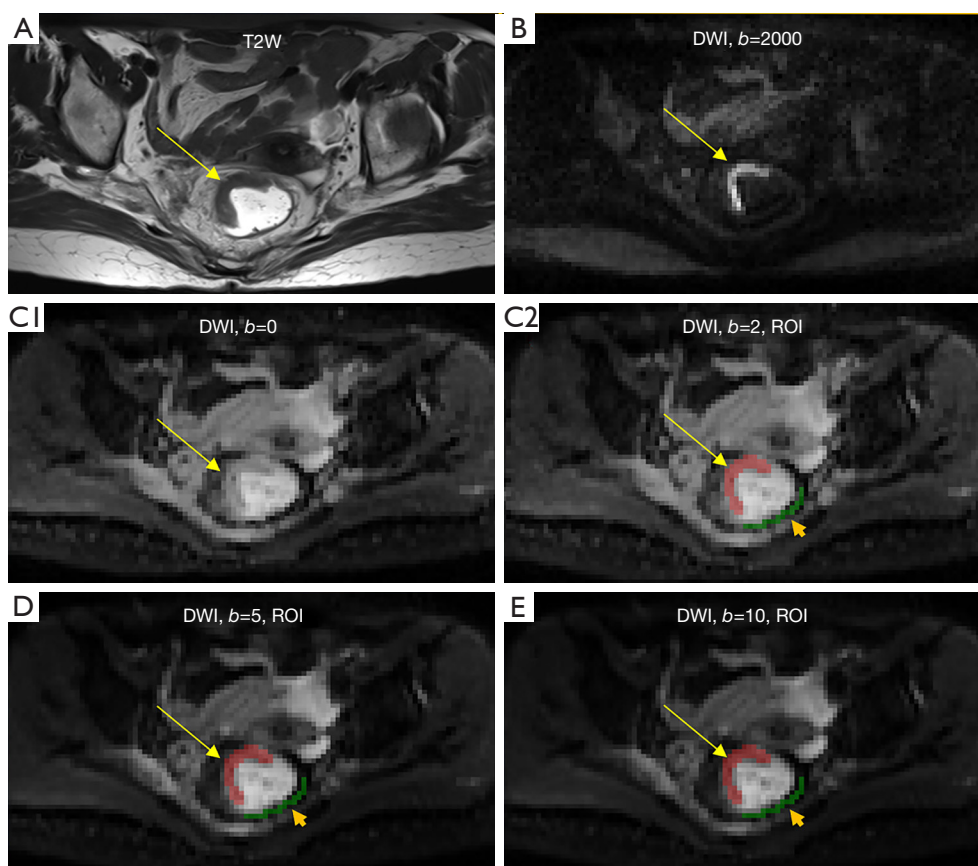
Figure 2 ROI segmentation of rectal carcinoma and tumor-free rectal wall for DDVD calculation. (A) T2-weighted anatomical image. (B-E) DWI acquired at b=2,000, b=0, b=5, and b=10 s/mm^2. Tumor region (long arrows) is identified with reference to anatomical image and b=2,000 image. ROI for rectal carcinoma (pixels in red color) or tumor-free rectal wall (short arrow, pixels in green color) was carefully drawn on b=0, b=5, and b=10 s/mm^2 images. T2W, T2-weighted; DWI, diffusion-weighted imaging; ROI, region-of-interest; DDVD, diffusion-derived vessel density.

acquired for each patient and the images were sufficient to cover the entirety of the RC in all cases. Diffusion images with three b-values of 0, 5, and 10 s/mm^2 were analysed in the current study.

DDVD measurement was conducted with Yingran Image Analytics software Diffeye version 1.0 (Yingran Medicals, Hong Kong SAR, China). Tumor border and tumor-free rectal wall were identified on standard anatomical T2-weighted image and a high b-value image. ROIs for both tumor and tumor-free rectal wall were segmented on the b=0 s/mm^2 image (resulting in ROI area of area0) and the b=5 (or 10) s/mm^2 image (resulting in ROI area of area5 or area10) respectively (*Figure 2*).

Two parameters were obtained as:

$$DDVD(b0b5) = Sb0/ROIarea0 - Sb5/ROIarea5$$
$$[\text{unit: arbitrary unit (au)/pixel}] \qquad [2]$$

$$DDVD(b0b10) = Sb0/ROIarea0 - Sb10/ROIarea10$$
$$[\text{unit: arbitrary unit (au)/pixel}] \qquad [3]$$

As absolute MR signal intensity is influenced by various factors, including B1 spatial inhomogeneity, coil loading, receiver gain, and DDVD measurement thresholding, etc., in this study the ratio of tumor DDVD to tumor-free rectal wall DDVD (DDVDr) was used to minimize these scaling factors. DDVDr was taken as:

$$DDVDr(b0b5) = [DDVD(b0b5) \text{ of RC}]/$$
$$[DDVD(b0b5) \text{ of rectal wall}] \qquad [4]$$

Table 1 DDVDr(b0b5) value of non-mucinous rectal carcinoma and mucinous rectal carcinoma

Classification	Non-mucinous tumor DDVDr(b0b5)				Mucinous tumor DDVDr(b0b5)			
	n	Mean	Median	95% CI	n	Mean	Median	95% CI
All	113	1.95	1.43	1.250–1.580	15	1.623	1.66	0.780–2.140
Clinical S*								
0&I	14	2.404	2.245	1.130–3.590	0	N/A	N/A	N/A
II	29	2.224	1.46	1.120–1.810	4	2.083	1.64	0.780–4.270
III	51	1.805	1.43	1.300–1.580	10	1.476	1.66	0.380–2.320
IV	11	1.434	1.13	0.930–2.120	1	1.25	1.25	N/A
Histological S								
W & m D	97	1.985	1.46	1.250–1.580	0	N/A	N/A	N/A
Poorly D	16	1.737	1.32	1.120–2.450	15	1.623	1.66	0.780–2.140
mrEMVI								
(–)	87	1.917	1.37	1.220–1.560	12	1.778	1.67	0.780–2.320
(+)	26	1.962	1.63	1.170–2.120	3	1.003	1.25	0.370–1.390

*, 8 patients lacking staging. DDVDr(b0b5), diffusion-derived vessel density ratio (RC to rectal wall) computed from b=0 and b=5 s/mm^2 diffusion weighted images; CI, confidence interval; Clinical S, clinical staging; N/A, not applicable; Histological S, histological staging; W & m D, well & moderately differentiated; Poorly D, poorly differentiated; mrEMVI, MRI-detected extramural vascular invasion; MRI, magnetic resonance imaging.

$$DDVDr(b0b10) = [DDVD(b0b10) \text{ of RC}] / [DDVD(b0b10) \text{ of rectal wall}] \quad [5]$$

Tumor and the corresponding tumor-free rectal wall were measured on all slices with measurable tumor size. The mean of all included slice measurements was then regarded as the value of the examination, with the last step weighted by the ROI area of each slice.

DDVD measures are presented in mean, median, and 95% confidence interval (CI). Statistical analysis was performed using GraphPad Prism Software (GraphPad Software Inc., San Diego, CA, USA). Comparisons between groups were tested by Kruskal-Wallis test. A P value <0.05 was considered statistically significant, >0.1 as not significant, and between 0.05 and 0.1 as with a trend of significance (as the current study was an exploratory study rather than a confirmatory study with pre-determined statistical power).

Results

The results are shown in *Table 1*, *Figures 3,4*. The median value of the DDVDr(b0b5) and DDVDr(b0b10) for non-mucinous RCs was 1.430 and 1.450 respectively, with the majority showing a higher DDVD than the adjacent tumor-free wall (i.e., with DDVDr >1). Based on DDVD(b0b5), 90.3% (102/113) of the non-mucinous RCs were hypervascular, 1.77% (2/113) were iso-vascular, and 7.96% (9/113) were hypovascular. The median value of the DDVDr(b0b5) and DDVDr(b0b10) for mucinous RCs was 1.660 and 1.670 respectively. Based on DDVDr(b0b5), 73.3% (11/15) were hypervascular, and 26.7% (4/15) were hypovascular. There was a very good correlation between DDVD(b0b5) and DDVD(b0b10) measures (Pearson r>0.93, *Figure 3*).

A trend was noted that earlier clinical grades non-mucinous RCs had a higher DDVDr(b0b5) than those of the advanced clinical grades (median: 2.245 for grade 0&I, 1.460 for grade II, 1.430 for grade III, 1.130 for grade IV, *Figure 4A,4B*). A non-significant trend was noted with well and moderately differentiated non-mucinous RCs having higher DDVDr(b0b5) than that of poorly differentiated non-mucinous RCs (median: 1.460 *vs.* 1.320, *Figure 4C*). A non-significant trend (P>0.1) was noted with mrEMVI positive non-mucinous RCs had higher DDVDr(b0b5) than that of mrEMVI negative non-mucinous RCs (1.630 *vs.* 1.370, *Figure 4D*). The sample size of mucinous RCs was too small to allow sub-group analysis.
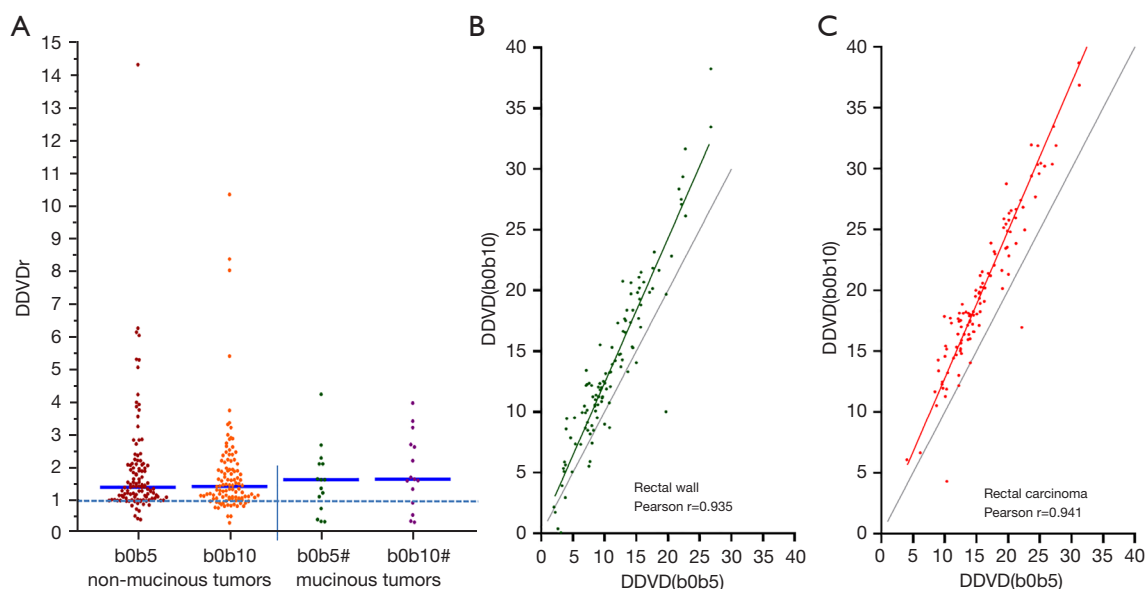
Figure 3 RC DDVDr value (A) and the correlation between DDVD(b0b5) and DDVD(b0b10). If the DDVDr is >1, then the tumor is hypervascular relative to rectal wall. If the ratio value is <1, then the tumor is hypovascular relative to rectal wall. For both non-mucinous RCs and mucinous RCs(#), the majority is hypervascular. DDVDr(b0b5) and DDVDr(b0b10) showed similar trends. B and C (non-mucinous RCs and the adjacent tumor-free rectal wall) show good correlation between DDVD(b0b5) and DDVD(b0b10) both for rectal wall and for RC. Grey lines indicate hypothetical 1-to-1 perfect correlation. Tissues on b=10 image are expected to have a lower signal than on b=5 image and thus DDVD(b0b10) will be larger than DDVD(b0b5), therefore on (B) and (C) the dots are mostly 'above' the grey line. The dots below the grey line present measurement imperfection. These dots are overall few and even fewer for RC measures than for rectal wall. This is understandable as rectal wall is thin and more difficult to measure [mucinous RCs and the adjacent tumor-free rectal wall show similar patterns as in (B) and (C)]. Bars in (A): median value. DDVDr, diffusion-derived vessel density ratio (RC to rectal wall); DDVD(b0b5), diffusion-derived vessel density computed from b=0 and b=5 s/mm^2 diffusion weighted images; DDVD(b0b10), diffusion-derived vessel density computed from b=0 and b=10 s/mm^2 diffusion weighted images; DDVDr(b0b5), diffusion-derived vessel density ratio (RC to rectal wall) computed from b=0 and b=5 s/mm^2 diffusion weighted images; RC, rectal carcinoma.

Discussion

Earlier perfusion CT studies demonstrated RC mostly has higher perfusion compared with that of tumor-free rectal wall. Sahani *et al.* (4) reported a blood flow (mL/100 g/min) of 31.02±15.55 for normal rectum wall and 60.33±29.13 for RC. Bellomi *et al.* (5) reported a blood flow (mL/100 g/min) of 20.8 (16.9, 38.2, median and 95% CI) for normal rectum wall and 65.4 (44.3, 107.0) for RC, a blood volume (mL/100 g) of 2.2 (1.7, 2.9) for normal rectum wall and 5.9 (4.5, 6.4) for RC. A graphic comparison of our results and the results of Sahani *et al.* and Bellomi *et al.* as shown in *Figure 5*, demonstrating good agreements in term of RC values relative to rectum wall value between DDVD results and CT results, though the exact correlation in the physiological meaning of DDVD measure and perfusion CT measure has not been established.

In the current study, a trend was noted that advanced clinical staging and poorer tumor differentiation of RC were associated with lower DDVD. This is consistent with earlier CT perfusion studies. Xu *et al.* (26) reported clinical staging I, II, III, and IV colorectal carcinomas had perfusion CT blood flow (mL/100 g/min) of 63.13±14.47, 41.52±12.31, 28.86±9.48, and 24.31±8.07 respectively (*Figure 6*). Hayano *et al.* (27) reported perfusion CT blood flow (mL/100 g/min) was 86.8±46.7 for well differentiated RCs and 64.1±39.3 for moderately differentiated RCs. Sun *et al.* (28) reported perfusion CT blood flow (mL/100 g/min) was 61.17±17.97 for well differentiated colorectal cancers, 34.80±13.06 for moderately differentiated colorectal cancers, and 22.24±9.31 for poorly differentiated colorectal cancers. Li *et al.* (29) reported perfusion CT blood flow (mL/100 g/min) was 47.33±8.49, 38.06±7.44, and 36.66±14.26 for Dukes' stage
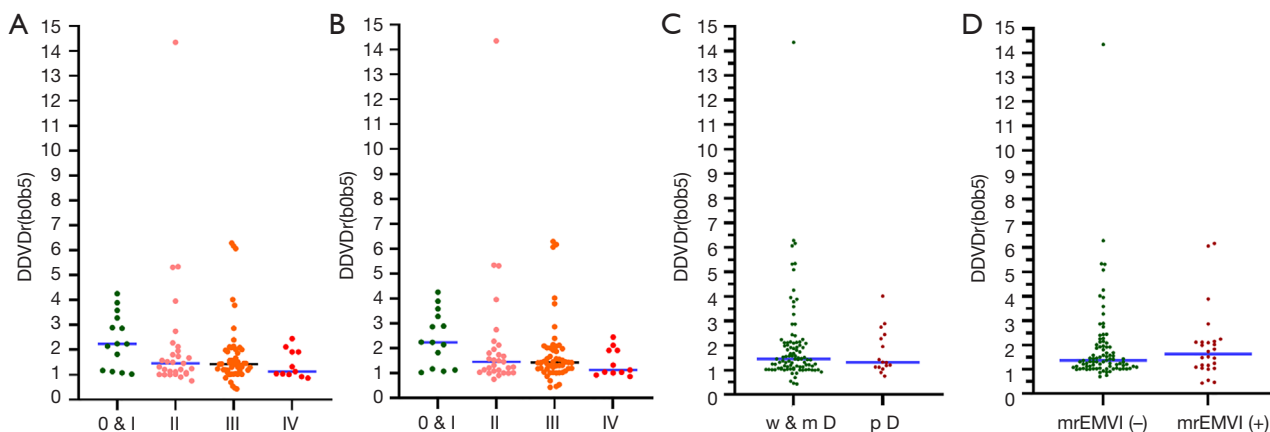
Figure 4 DDVDr according to tumor classification. A marginally significant trend (Kruskal-Wallis test) was noted for clinically advanced tumors [(A) excluding mucinous tumors, P=0.09; (B) including mucinous tumors, P=0.08] associated with lower DDVDr. (C) A non-significant trend was noted with p D non-mucinous tumors had lower DDVDr than that of the w & m D non-mucinous tumors; and (D) a non-significant trend was noted with mrEMVI (+) non-mucinous tumors had higher DDVDr than that of mrEMVI (–) non-mucinous tumors. Bars: median value. DDVDr(b0b5), diffusion-derived vessel density ratio (RC to rectal wall) computed from $b=0$ and $b=5$ s/mm^2 diffusion weighted images; mrEMVI, MRI-detected extramural vascular invasion; w & m D, well and moderately differentiated; p D, poorly differentiated; RC, rectal carcinoma; MRI, magnetic resonance imaging.

A, B, and C tumors (30), respectively. In colorectal cancer, Goh *et al.* (6) reported that tumor blood flow measured by perfusion CT was significantly lower in patients who ultimately developed metastatic disease.

Results from DCE and IVIM MRI studies have been more mixed. Yeo *et al.* (7) reported Ktrans (min^{-1}) showed a significant inverse correlation with T staging, with T1 tumor having a value of 0.132±0.080 and T2–4 tumor having a value of 0.104±0.030. Ciolina *et al.* (8) reported Kep (min^{-1}) of RC was 1.08±0.80, 0.58±0.52, 0.26±0.22, for well differentiated, moderately differentiated, and poorly differentiated RCs, respectively. Therefore, the DDVD results in the current study are consistent with the results of Yeo *et al.* (7) and Ciolina *et al.* (8) in trend. Shen *et al.* (31) reported that Ktrans (min^{-1}) was 0.118±0.032 for rectum wall and 0.267±0.071 for RC; however, they reported Ktrans for well differentiated RCs to be 0.182±0.153, for moderately differentiated RCs to be 0.280±0.067, and for poorly differentiated RCs to be 0.284±0.068. Lu *et al.* (10) reported IVIM PF was 0.18±0.09 for rectal wall and 0.13±0.03 for RC (this is the opposite of expectation); and PF was 0.14±0.03 for well/moderately differentiated RCs, and 0.12±0.04 for poorly differentiated RCs. Sun *et al.* (32) reported IVIM PF was 0.33±0.069 for well differentiated RCs, 0.26±0.059 for moderately differentiated RCs, and 0.24±0.0569 for poorly differentiated RCs (these

PF values are exceedingly high). Surov *et al.* (9) reported there was no statistically significant difference in IVIM PF for moderately differentiated RCs (0.184±0.072) and poorly differentiated RCs (0.194±0.068), but with PF being slightly higher for poorly differentiated RCs. It has been recognized that both DCE-MRI and IVIM imaging can derive unstable results (33-36). Moreover, recent studies showed that in addition to physiological perfusion, IVIM PF is also heavily affected by tissue's T2 time, with longer T2 time leading to a 'depressed' PF measure (37). For example, HCCs mostly show higher perfusion values compared with the adjacent normal liver tissue, reflecting their hypervascular nature (19,20). Paradoxically, most authors reported a decreased PF of HCC relative to the adjacent liver [such as: Penner *et al.* (38): 0.09 *vs.* 0.18; Zhu *et al.* (39): 0.14 *vs.* 0.22; Woo *et al.* (40): 0.22 *vs.* 0.25; Shan *et al.* (41): 0.19 *vs.* 0.22; Hectors *et al.* (42): 0.18 *vs.* 0.23]. In contrast to perfusion CT results and DDVD results in this study, IVIM-PF had been measured *lower* for RC than in tumor-free rectal wall (10). Both for the case of HCC and RC, lower IVIM PF in the tumor than in adjacent normal tissue could be due to the increased T2 relaxation time of the tumor (37).

There are many limitations to this study. This is a preliminary proof-of-concept study for DDVD application in RC perfusion assessment, whereas the DDVD protocol was not optimized. Though no difference was detected for
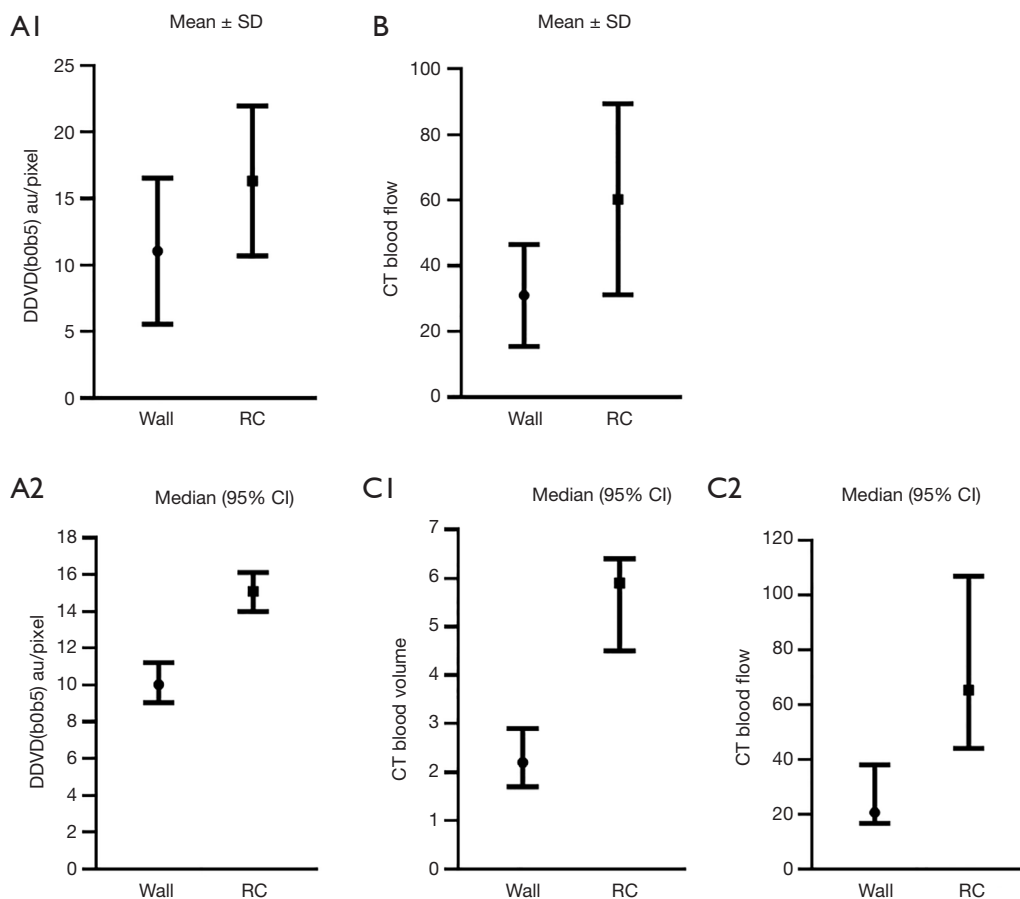
Figure 5 A graphic comparison of DDVD results in this study [(A1) and (A2), unit: arbitrary unit (au)/pixel] and (B) the perfusion CT blood flow (mL/100 g/min) and/or blood volume (mL/100 g) results of (A) Sahani *et al.* (4) and (C1,C2) Bellomi *et al.* (5). CT data are re-plotted from (4,5). SD, standard deviation; DDVD(b0b5), diffusion-derived vessel density computed from $b=0$ and $b=5$ s/mm^2 diffusion weighted images; Wall, tumor-free rectal wall; RC, rectal carcinoma; CI, confidence interval; DDVD, diffusion-derived vessel density; CT, computed tomography.

DDVD(b0b5) and DDVD(b0b10) in this study, our earlier study showed that DDVD(b0b2) is better in assessing hepatocellular carcinoma than DDVD(b0b10), which is consistent with the initial definition of DDVD (11). The data were initially acquired for IVIM analysis. Our recent experience shows increasing NEX can improve DDVD measure stability (i.e., repeatability and reproducibility), and since the DDVD protocol is very fast, higher NEX will be practically feasible. Drawing ROIs along rectal wall is difficult and can be contaminated by the partial volume effect. The DDVD difference between histological gradings and between mrEMVI (–) and mrEMVI (+) cases were both not statistically significant. This on one side reflects the magnitudes of the differences were small, on the other side reflects our study was not statistically powered to detect these differences. In one patient, tumor-free rectal

wall signals at $b=5$ and 10 s/mm^2 images were higher than tumor-free rectal wall signal at $b=0$ images, thus data of this patient was excluded from analysis. That tumor-free rectal wall signal at $b=5$ and 10 mm^2/s image being higher than tumor-free rectal wall signal at $b=0$ mm^2/s image would be unreasonable. MRI signal is affected by many factors including motion artifacts and scaling factor. Again, increasing the NEX will be one of the means to overcome measurement instabilities. Another limitation is that we had only 15 patients with mucinous RC, thus subgroup analysis for mucinous RCs was not feasible.

Conclusions

In conclusion, DDVD analysis suggests that the majority of RCs are hypervascular. RC's DDVD results appear to agree

3272

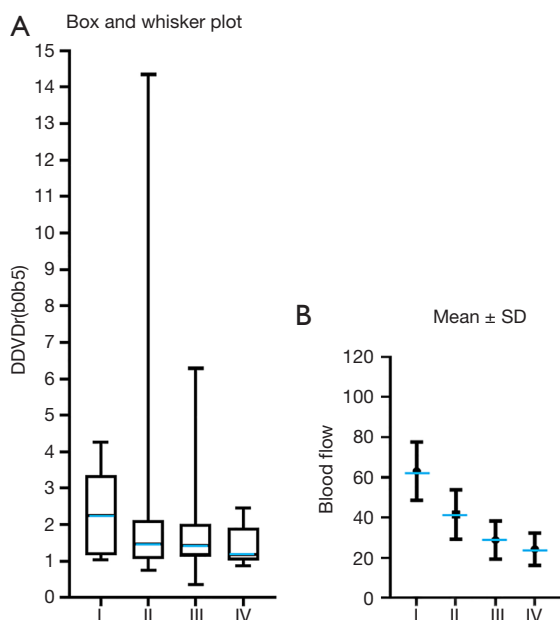**Lu et al. Rectum carcinoma perfusion by DDVD**

Figure 6 A graphic comparison of rectal carcinoma DDVD results in the current study (A) and the perfusion CT blood flow (mL/100 g/min) colorectal carcinoma results of (B) Xu *et al.* (26). Data in (A) included both non-mucinous and mucinous tumors. Including or excluding mucinous tumors does not affect the trend patter in (A). Blue bar: median in (A) and mean in (B). CT data are re-plotted from (26). DDVDr(b0b5), diffusion-derived vessel density ratio (RC to rectal wall) computed from b=0 and b=5 s/mm^2 diffusion weighted images; SD, standard deviation; DDVD, diffusion-derived vessel density; CT, computed tomography; RC, rectal carcinoma.

with literature CT perfusion results which have been more consistent compared with DCE MRI or IVIM literature results. Our future studies will include the evaluation of DDVD pixelwise mapping (43). Upon further technical optimizations, DDVD may be a clinically applicable imaging biomarker for RC perfusion assessment.

Acknowledgments

Footnote

Conflicts of Interest: All authors have completed the ICMJE uniform disclosure form (available at https://qims.amegroups.com/article/view/10.21037/qims-24-406/coif).

Y.X.J.W. serves as the Editor-in-Chief of *Quantitative Imaging in Medicine and Surgery*. He is the founder of Yingran Medicals Ltd., which develops medical image-based diagnostics software. The other authors have no conflicts of interest to declare.

Ethical Statement: The authors are responsible for ensuring that all aspects of the work are investigated and resolved concerning questions regarding accuracy or integrity. The study was conducted in accordance with the Declaration of Helsinki (as revised in 2013). The conduct of the study was approved by the local institutional ethical committee, and informed consent was obtained for all study subjects.

References

1. Weidner N. Intratumor microvessel density as a prognostic factor in cancer. Am J Pathol 1995;147:9-19.
2. Tanigawa N, Amaya H, Matsumura M, Lu C, Kitaoka A, Matsuyama K, Muraoka R. Tumor angiogenesis and mode of metastasis in patients with colorectal cancer. Cancer Res 1997;57:1043-6.
3. Choi HJ, Hyun MS, Jung GJ, Kim SS, Hong SH. Tumor angiogenesis as a prognostic predictor in colorectal carcinoma with special reference to mode of metastasis and recurrence. Oncology 1998;55:575-81.
4. Sahani DV, Kalva SP, Hamberg LM, Hahn PF, Willett CG, Saini S, Mueller PR, Lee TY. Assessing tumor perfusion and treatment response in rectal cancer with multisection CT: initial observations. Radiology 2005;234:785-92.
5. Bellomi M, Petralia G, Sonzogni A, Zampino MG, Rocca A. CT perfusion for the monitoring of neoadjuvant chemotherapy and radiation therapy in rectal carcinoma: initial experience. Radiology 2007;244:486-93.
6. Goh V, Halligan S, Wellsted DM, Bartram CI. Can perfusion CT assessment of primary colorectal adenocarcinoma blood flow at staging predict for

subsequent metastatic disease? A pilot study. Eur Radiol 2009;19:79-89.

7. Yeo DM, Oh SN, Jung CK, Lee MA, Oh ST, Rha SE, Jung SE, Byun JY, Gall P, Son Y. Correlation of dynamic contrast-enhanced MRI perfusion parameters with angiogenesis and biologic aggressiveness of rectal cancer: Preliminary results. J Magn Reson Imaging 2015;41:474-80.

8. Ciolina M, Caruso D, De Santis D, Zerunian M, Rengo M, Alfieri N, Musio D, De Felice F, Ciardi A, Tombolini V, Laghi A. Dynamic contrast-enhanced magnetic resonance imaging in locally advanced rectal cancer: role of perfusion parameters in the assessment of response to treatment. Radiol Med 2019;124:331-8.

9. Surov A, Meyer HJ, Höhn AK, Behrmann C, Wienke A, Spielmann RP, Garnov N. Correlations between intravoxel incoherent motion (IVIM) parameters and histological findings in rectal cancer: preliminary results. Oncotarget 2017;8:21974-83.

10. Lu B, Yang X, Xiao X, Chen Y, Yan X, Yu S. Intravoxel Incoherent Motion Diffusion-Weighted Imaging of Primary Rectal Carcinoma: Correlation with Histopathology. Med Sci Monit 2018;24:2429-36.

11. Wáng YXJ. Living tissue intravoxel incoherent motion (IVIM) diffusion MR analysis without b=0 image: an example for liver fibrosis evaluation. Quant Imaging Med Surg 2019;9:127-33.

12. Xiao BH, Huang H, Wang LF, Qiu SW, Guo SW, Wáng YXJ. Diffusion MRI Derived per Area Vessel Density as a Surrogate Biomarker for Detecting Viral Hepatitis B-Induced Liver Fibrosis: A Proof-of-Concept Study. SLAS Technol 2020;25:474-83.

13. Hu GW, Zheng CJ, Zhong WX, Zhuang DP, Xiao BH, Wáng YXJ. Usefulness of diffusion derived vessel density computed from a simplified IVIM imaging protocol: An experimental study with rat biliary duct blockage induced liver fibrosis. Magn Reson Imaging 2021;84:115-23.

14. Zheng CJ, Huang H, Xiao BH, Li T, Wang W, Wáng YXJ. Spleen in viral Hepatitis-B liver fibrosis patients may have a reduced level of per unit micro-circulation: non-invasive diffusion MRI evidence with a surrogate marker. SLAS Technol 2022;27:187-94.

15. Huang H, Zheng CJ, Wang LF, Che-Nordin N, Wáng YXJ. Age and gender dependence of liver diffusion parameters and the possibility that intravoxel incoherent motion modeling of the perfusion component is constrained by the diffusion component. NMR Biomed 2021;34:e4449.

16. Li XM, Yao DQ, Quan XY, Li M, Chen W, Wáng YXJ. Perfusion of hepatocellular carcinomas measured by diffusion-derived vessel density biomarker: Higher hepatocellular carcinoma perfusion than earlier intravoxel incoherent motion reports. NMR Biomed 2024. [Epub ahead of print]. doi: 10.1002/nbm.5125.

17. He J, Chen C, Xu L, Xiao B, Chen Z, Wen T, Wáng YXJ, Liu P. Diffusion-Derived Vessel Density Computed From a Simplified Intravoxel Incoherent Motion Imaging Protocol in Pregnancies Complicated by Early Preeclampsia: A Novel Biomarker of Placental Dysfunction. Hypertension 2023;80:1658-67.

18. Lu T, Wang L, Li M, Wang Y, Chen M, Xiao BH, Wáng YXJ. Diffusion-derived vessel density (DDVD) computed from a simple diffusion MRI protocol as a biomarker of placental blood circulation in patients with placenta accreta spectrum disorders: A proof-of-concept study. Magn Reson Imaging 2024;109:180-6.

19. Sahani DV, Holalkere NS, Mueller PR, Zhu AX. Advanced hepatocellular carcinoma: CT perfusion of liver and tumor tissue--initial experience. Radiology 2007;243:736-43.

20. Abdullah SS, Pialat JB, Wiart M, Duboeuf F, Mabrut JY, Bancel B, Rode A, Ducerf C, Baulieux J, Berthezene Y. Characterization of hepatocellular carcinoma and colorectal liver metastasis by means of perfusion MRI. J Magn Reson Imaging 2008;28:390-5.

21. American Joint Committee on Cancer (AJCC), 8th edition. Available online: https://www.facs.org/quality-programs/cancer-programs/american-joint-committee-on-cancer/. Accepted on 12th Dec 2023.

22. Compton CC, Henson DE, Hutter RV, Sobin LH, Bowman HE. Updated protocol for the examination of specimens removed from patients with colorectal carcinoma. A basis for checklists. Arch Pathol Lab Med 1997;121:1247-54.

23. Smith NJ, Barbachano Y, Norman AR, Swift RI, Abulafi AM, Brown G. Prognostic significance of magnetic resonance imaging-detected extramural vascular invasion in rectal cancer. Br J Surg 2008;95:229-36.

24. Chen S, Li N, Tang Y, Shi J, Zhao Y, Ma H, Wang S, Li YX, Jin J. The prognostic value of MRI-detected extramural vascular invasion (mrEMVI) for rectal cancer patients treated with neoadjuvant therapy: a meta-analysis. Eur Radiol 2021;31:8827-37.

25. McCawley N, Clancy C, O'Neill BD, Deasy J, McNamara DA, Burke JP. Mucinous Rectal Adenocarcinoma Is Associated with a Poor Response to Neoadjuvant Chemoradiotherapy: A Systematic Review and Meta-analysis. Dis Colon Rectum 2016;59:1200-8.

3274

Lu et al. Rectum carcinoma perfusion by DDVD

26. Xu Y, Sun H, Song A, Yang Q, Lu X, Wang W. Predictive Significance of Tumor Grade Using 256-Slice CT Whole-Tumor Perfusion Imaging in Colorectal Adenocarcinoma. Acad Radiol 2015;22:1529-35.

27. Hayano K, Shuto K, Koda K, Yanagawa N, Okazumi S, Matsubara H. Quantitative measurement of blood flow using perfusion CT for assessing clinicopathologic features and prognosis in patients with rectal cancer. Dis Colon Rectum 2009;52:1624-9.

28. Sun H, Xu Y, Yang Q, Wang W. Assessment of tumor grade and angiogenesis in colorectal cancer: whole-volume perfusion CT. Acad Radiol 2014;21:750-7.

29. Li ZP, Meng QF, Sun CH, Xu DS, Fan M, Yang XF, Chen DY. Tumor angiogenesis and dynamic CT in colorectal carcinoma: radiologic-pathologic correlation. World J Gastroenterol 2005;11:1287-91.

30. Available online: https://www.cancerresearchuk.org/about-cancer/bowel-cancer/stages-types-and-grades/dukes-staging. Accessed on 12th Dec 2023.

31. Shen FU, Lu J, Chen L, Wang Z, Chen Y. Diagnostic value of dynamic contrast-enhanced magnetic resonance imaging in rectal cancer and its correlation with tumor differentiation. Mol Clin Oncol 2016;4:500-6.

32. Sun H, Xu Y, Song A, Shi K, Wang W. Intravoxel Incoherent Motion MRI of Rectal Cancer: Correlation of Diffusion and Perfusion Characteristics With Prognostic Tumor Markers. AJR Am J Roentgenol 2018;210:W139-47.

33. Galbraith SM, Lodge MA, Taylor NJ, Rustin GJ, Bentzen S, Stirling JJ, Padhani AR. Reproducibility of dynamic contrast-enhanced MRI in human muscle and tumours: comparison of quantitative and semi-quantitative analysis. NMR Biomed 2002;15:132-42.

34. Huang W, Chen Y, Fedorov A, Li X, Jajamovich GH, Malyarenko DI, et al. The Impact of Arterial Input Function Determination Variations on Prostate Dynamic Contrast-Enhanced Magnetic Resonance Imaging Pharmacokinetic Modeling: A Multicenter Data Analysis Challenge, Part II. Tomography 2019;5:99-109.

35. Debus C, Floca R, Nörenberg D, Abdollahi A, Ingrisch M. Impact of fitting algorithms on errors of parameter estimates in dynamic contrast-enhanced MRI. Phys Med Biol 2017;62:9322-40.

36. Wang YXJ, Huang H, Zheng CJ, Xiao BH, Chevallier O, Wang W. Diffusion-weighted MRI of the liver: challenges and some solutions for the quantification of apparent diffusion coefficient and intravoxel incoherent motion. Am

J Nucl Med Mol Imaging 2021;11:107-42.

37. Ma FZ, Wáng YXJ. T2 relaxation time elongation of hepatocellular carcinoma relative to native liver tissue leads to an underestimation of perfusion fraction measured by standard intravoxel incoherent motion magnetic resonance imaging. Quant Imaging Med Surg 2024;14:1316-22.

38. Penner AH, Sprinkart AM, Kukuk GM, Gütgemann I, Gieseke J, Schild HH, Willinek WA, Mürtz P. Intravoxel incoherent motion model-based liver lesion characterisation from three b-value diffusion-weighted MRI. Eur Radiol 2013;23:2773-83.

39. Zhu L, Cheng Q, Luo W, Bao L, Guo G. A comparative study of apparent diffusion coefficient and intravoxel incoherent motion-derived parameters for the characterization of common solid hepatic tumors. Acta Radiol 2015;56:1411-8.

40. Woo S, Lee JM, Yoon JH, Joo I, Han JK, Choi BI. Intravoxel incoherent motion diffusion-weighted MR imaging of hepatocellular carcinoma: correlation with enhancement degree and histologic grade. Radiology 2014;270:758-67.

41. Shan Y, Zeng MS, Liu K, Miao XY, Lin J, Fu Cx, Xu PJ. Comparison of Free-Breathing With Navigator-Triggered Technique in Diffusion Weighted Imaging for Evaluation of Small Hepatocellular Carcinoma: Effect on Image Quality and Intravoxel Incoherent Motion Parameters. J Comput Assist Tomogr 2015;39:709-15.

42. Hectors SJ, Wagner M, Besa C, Bane O, Dyvorne HA, Fiel MI, Zhu H, Donovan M, Taouli B. Intravoxel incoherent motion diffusion-weighted imaging of hepatocellular carcinoma: Is there a correlation with flow and perfusion metrics obtained with dynamic contrast-enhanced MRI? J Magn Reson Imaging 2016;44:856-64.

43. Yao DQ, Zheng CJ, Deng YY, Lu BL, Lu T, Hu GW, Li XM, Xiao BH, Ma FZ, Sabarudin A, King AD, Wáng YXJ. Potential diverse applications of diffusion-derived vessel density (DDVD) pixel-by-pixel mapping. Quant Imaging Med Surg 2024;14:2136-45.
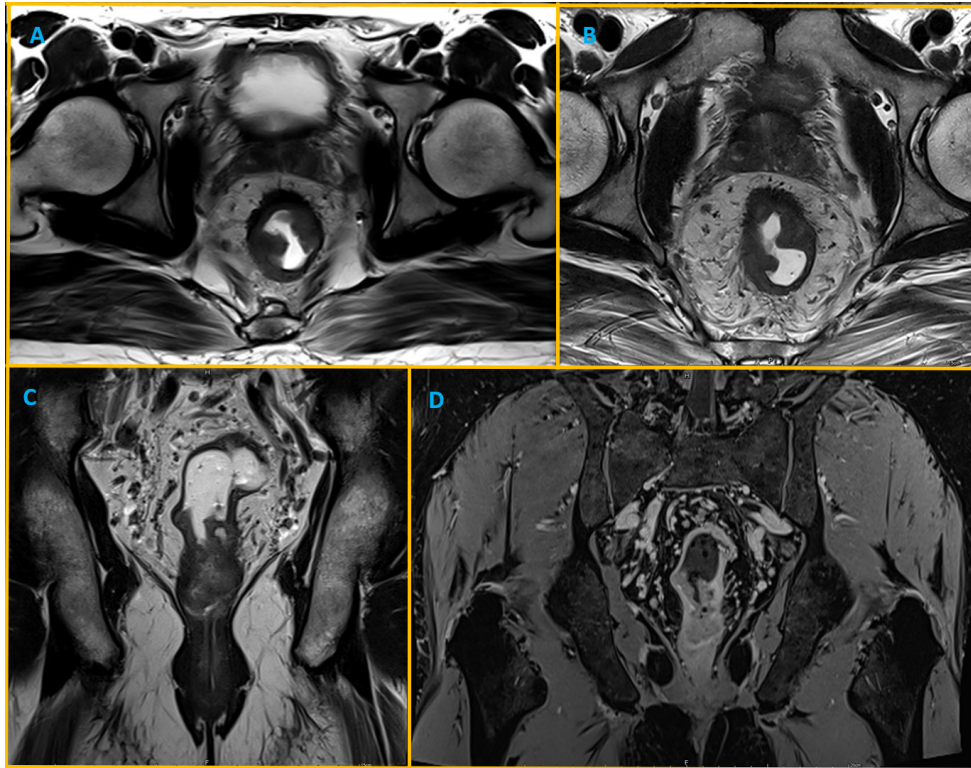
Figure S1 A rectal carcinoma patient without mrEMVI. (A,B) T2-weighted axial images; (C) T2-weighted coronal image; (D) T1-weighted Gadolinium enhanced coronal image. mrEMVI, MRI-detected extramural vascular invasion; MRI, magnetic resonance imaging.
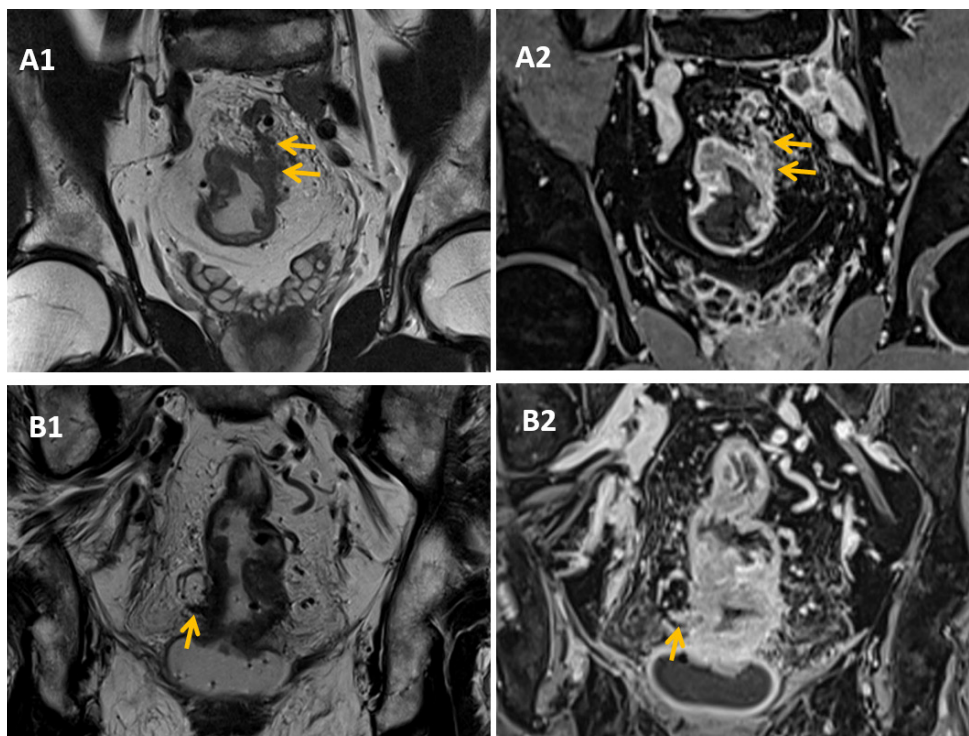

Figure S2 Two rectal carcinoma patients with mrEMVI (arrows). (A1,B1) T2-weighted coronal images. (A2,B2) T1 weighted Gadolinium enhanced coronal image. (A1) and (A2) are one patient, and (B1) and (B2) are one patient. mrEMVI, MRI-detected extramural vascular invasion; MRI, magnetic resonance imaging.